INTERFEROMETRIC MEASUREMENT OF MICROWAVE HELICON DISPERSION AND THE HOLE DAMPING EFFECT IN INTRINSIC InSb

Jacek K. Furdyna

National Magnet Laboratory,* Massachusetts Institute of Technology, Cambridge, Massachusetts
(Received 2 March 1965)

Helicon wave propagation was investigated in intrinsic InSb at 35 Gc/sec in the temperature range from 200 to 400°K in magnetic fields up to 100 kG. In this range InSb affords an opportunity to study electromagnetic wave interaction with a fast plasma of electrons moving in a much slower hole plasma, rather than in the usual fixed ion background. Well-defined Rayleigh-type interference patterns, obtainable even at the highest temperatures of the investigated range, indicate that the hole contribution to the helicon dispersion is negligible in practically the entire available field region, and in this sense the role of the slow carriers is similar to that of fixed positive ions. However, even at moderate fields, the hole plasma provides the dominant damping mechanism of the helicons, manifested by a radical truncation of the interference pattern at $B \approx 1.7 \times (\mu_h \mu_e)^{-1/2}$, where μ_h and μ_e are the hole and electron mobilities. The envelope of the interference pattern can then be used to measure the mobilities of both carrier species. Our results, obtained by using the classical helicon model, are in reasonable, though not spectacular, agreement (≈25%) with the known dc mobilities, and point to the inadequacy of the model in the proximity of the quantum regime as a likely cause for the discrepancy. Rayleigh patterns have also been obtained by varying the concentration via temperature at fixed field. This provides a method of direct, quick, and precise determination of carrier concentration and magnetoconductivity as a function of temperature. The agreement between the results and the known temperature dependence of the intrinsic concentration in InSb is excellent. A microwave analog of the Rayleigh refractometer was used to study the above phenomena. This approach is in many ways superior to the Fabry-Perot dimensional resonance technique used in previous helicon experiments in this frequency range, particularly where considerable losses are involved. It provides, for the first time in semiconducting plasmas, a means of determining the helicon dispersion relation with precision comparable to that attained at lower frequencies in metals,[1] and in addition can be used for quantitative study of damping processes.

Propagation constants for the helicon mode in an intrinsic material characterized by the conditions $\mu_e B \equiv \theta_e \gg 1$, $\mu_h B \equiv \theta_h \ll 1$ have been given by Libchaber and Veilex in terms of the classical model.[2] We merely generalize their expressions to energy-dependent statistics, and retain higher order terms which are important at high fields. Thus the phase constant becomes

$$\alpha = \frac{2\pi}{\lambda} = \left(\frac{\omega \mu_0 n_i e}{B}\right)^{1/2} \left\langle 1 - \frac{\theta_h^2}{2} \right\rangle \text{ (mks units)}, \quad (1)$$

and the associated attenuation coefficient

$$\beta = \frac{1}{2}\left(\frac{\omega \mu_0 n_i e}{B}\right)^{1/2} \times \left[\left\langle \frac{1}{\theta_e} \right\rangle + \langle \theta_h (1 - \theta_h^2) \rangle\right] \left\langle 1 + \frac{\theta_h^2}{2} \right\rangle. \quad (2)$$

Here λ is the wavelength in the medium, ω the angular frequency, μ_0 the permeability of free space, n_i the intrinsic concentration, and e the electronic charge, and the angular brackets denote Boltzmann averages. The second term in the square brackets of Eq. (2) is the hole damping term, which truncates the helicon amplitude at higher fields.

Earlier observations of the oscillatory nature of microwave transmission through intrinsic InSb were made at 195°K by the author, who at that time described the phenomenon empirically.[3] Libchaber and Veilex[2] have introduced the classical dispersion relation for the intrinsic case and have observed the effect at room temperature. Their work has demonstrated the basic features of helicon propagation in fields below the onset of hole damping, and they were able to obtain a quantitative estimate of n_i despite the limitations inherent in the Fabry-

Perot technique under conditions of severe attenuation.

In the present experiment a microwave version of the classical Rayleigh refractometer was used. This approach is basically analogous to the "leakage" technique used in microwave Alfvén wave measurements in Bi,[4] and in radio-frequency helicon experiments in metals.[5] The arrangement consists essentially of a microwave bridge, one arm containing a circular polarizer and the sample placed in a cylindrical wave guide concentric with a Bitter solenoid, and the other arm containing an attenuator and a phase shifter. The power in the reference arm considerably exceeds the power transmitted through the sample. The interference condition for the present arrangement is $(\delta + N)\lambda = d$, where N is an integer, d is the thickness of the specimen, and δ is a constant depending on the phase-shifter setting. The interference pattern is periodic in $B^{-1/2}$, with the period Δ given by

$$\Delta = (2\pi/d)(\omega\mu_0 n_i e)^{-1/2}. \quad (3)$$

When, as in the case at hand, multiple reflections can be ignored due to high attenuation within the specimen, the amplitude of the interference pattern is, to first order in θ_h,

$$E = 4\frac{\lambda}{\lambda_0}E_0 \exp(-\beta d)$$
$$= 4\frac{\lambda}{\lambda_0}E_0 \exp\left(-\frac{\pi}{\Delta}\left\langle\frac{1}{\mu_e B^{3/2}} + \mu_h B^{1/2}\right\rangle\right), \quad (4)$$

where E_0 is the incident amplitude, λ_0 the free-space wavelength, and the factor $4(\lambda/\lambda_0)$ is the transmission modulus across the two boundaries. The latter quantity must be taken into account since, through Eq. (1), it is B dependent. By measuring the period and taking the logarithm of the amplitude at three fields, the parameters in Eqs. (3) and (4) are, in principle, determined. In particular, it can easily be seen that the envelope of an interference pattern will exhibit a "knee" when $\mu_e\mu_h B^2 \approx 3$. Note that d is eliminated in Eq. (4) through a measurement of Δ, and quantitative experiments may therefore be conducted on samples with nonparallel faces or unknown thicknesses. Since the technique does not rely on multiple reflections, it can be used to study highly attenuating specimens. The unbalanced bridge is, of course, basically a microwave phase detector. With the arrangement as described, signals in the sample arm 40 dB below noise level could be observed under conditions of high bridge unbalance, and this figure was further significantly improved by modulation of the signal in the sample arm and synchronous detection. A very significant feature of the highly unbalanced bridge is also the fact that the envelope amplitude is proportional to the first power of the transmitted amplitude regardless of the power response of the detector, thus making the technique particularly suitable for the study of damping processes.[6]

Figure 1 serves to illustrate several features

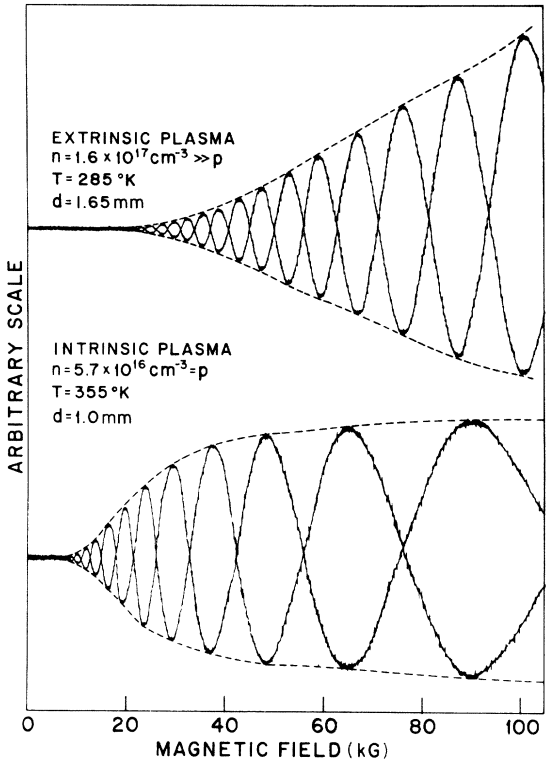

FIG. 1. X-Y recorder traces of Rayleigh-type interference patterns as a function of magnetic field, contrasting helicon propagation in extrinsic and intrinsic media. The overlapping curves represent consecutive sweeps corresponding to 180° out-of-phase settings of the interferometer bridge. The upper curve, obtained with highly doped n-type InSb, illustrates the familiar case of propagation through an electron plasma moving in the background of fixed positive ions. The strikingly different behavior of the intrinsic case, where the electron plasma moves in the background of comparatively heavy (but not localized) holes, is shown below. In the latter case, the hole background does not contribute appreciably to the period except at the highest fields, but provides the major damping mechanism at moderate fields, radically truncating the helicon amplitude beyond ca. 20 kG.

of the Rayleigh-type experiment and to contrast the behavior of hole-damped helicon propagation through intrinsic material with the behavior in extrinsic plasmas. The upper curve was obtained with a heavily doped n-type InSb sample at 285°K, and the lower one with pure InSb at 355°K. The overlapping curves represent two consecutive sweeps obtained by changing the phase in one of the bridge arms by 180°. Note that the crossover points provide an extremely precise method of determining the helicon phase velocity. Note further that an arbitrary number of such crossover points can be generated by appropriate phase settings, and can be used to determine the dispersion relation even under conditions when less than one complete oscillation can be observed. The latter feature emphasizes the basic similarity of the helicon phenomenon and the high-field Faraday rotation.[7] Note finally the striking contrast between the envelope of the interference pattern for an intrinsic plasma, truncated by the onset of hole damping (shown in the lower curve), and the typical uniformly rising envelope of an extrinsic plasma (upper curve).[8]

Figure 2 shows Rayleigh patterns obtained for pure InSb at three temperatures in the intrinsic range. The concentrations indicated are in excellent agreement with the relation $n_i^2 = 3.6T^3 \exp(-0.26/kT)$ giving the intrinsic concentration in this material.[9] At the highest fields the periodicity of the interference pattern is slightly, but observably, affected by the hole contribution to the helicon dispersion [see Eq. (1)], marking the beginning of a gradual transition to the (damped) Alfvén wave mode. Note the increasing amplitude in the high-field limit, particularly pronounced at lower temperatures, arising due to the θ_h^2 terms which tend to decrease the effect of the hole damping term in Eq. (2). A quantitative analysis of the envelopes of the interference patterns at various temperatures throughout the intrinsic range consistently yields the quantity $e/(m_e^*\langle\tau_e^{-1}\rangle)$ higher than the known electron mobility by ca. 20 to 30% and $e\langle\tau\rangle/m_h^*$ lower by a comparable amount than the corresponding hole mobility. The room-temperature values thus obtained are $e/(m_e^*\langle\tau_e^{-1}\rangle) \approx 9.5$ and $e\langle\tau\rangle/m_h^* \approx 0.55$ m^2/V sec, compared with typical dc values of 7.8 and 0.075 m^2/V sec, respectively.[9] This discrepancy points to the inadequacy of the model used, since, unlike dispersion, the absorption term is not free from quantum effects, affecting m_e^* and τ_e as well as the statistics involved in the τ averages to a varying degree as the field is increased.[10] Although the quantum limit $\hbar\omega_{ce} = kT$ is not reached, the electron-cyclotron frequency ω_{ce} is sufficiently high to account for some departure from the purely classical case. It must be remembered that the success of the classical plasma model in predicting the correct helicon dispersion is somewhat fortuitous, arising from a fortunate cancellation of the terms affected by the quantum contributions in the expression for the high-field dielectric constant. The same degree of success is therefore not expected in describing the associated losses. A more rigorous theoretical formulation applicable to the present case is currently being developed.

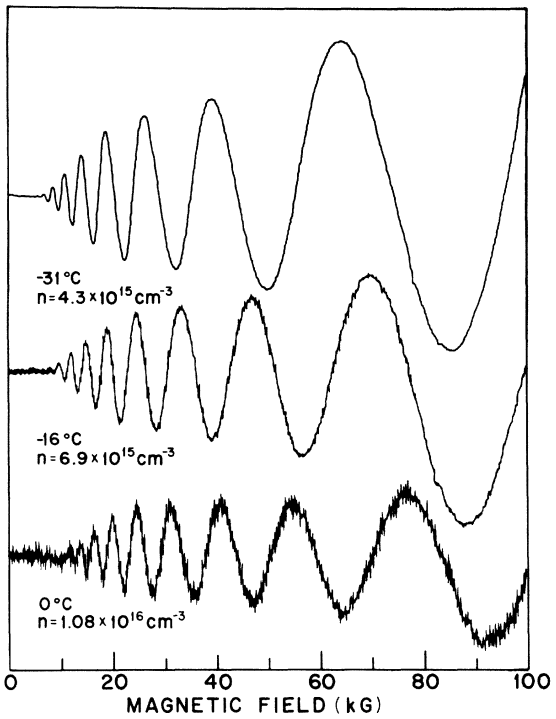

FIG. 2. Recorder traces of helicon interference patterns in intrinsic InSb observed at temperatures indicated using a 35-Gc/sec microwave bridge. The sample thickness was 4.32 mm. The electron concentrations shown were calculated from the observed period, and are in excellent agreement with the known intrinsic values. Note the truncation of the amplitude due to hole damping. Note also that the "flat" portion of the curves is shortened as the temperature decreases due to the increasing importance of quadratic $\mu_h B$ terms at high fields [cf. Eq. (2)].

In an intrinsic semiconductor the helicon dispersion varies rapidly with temperature through

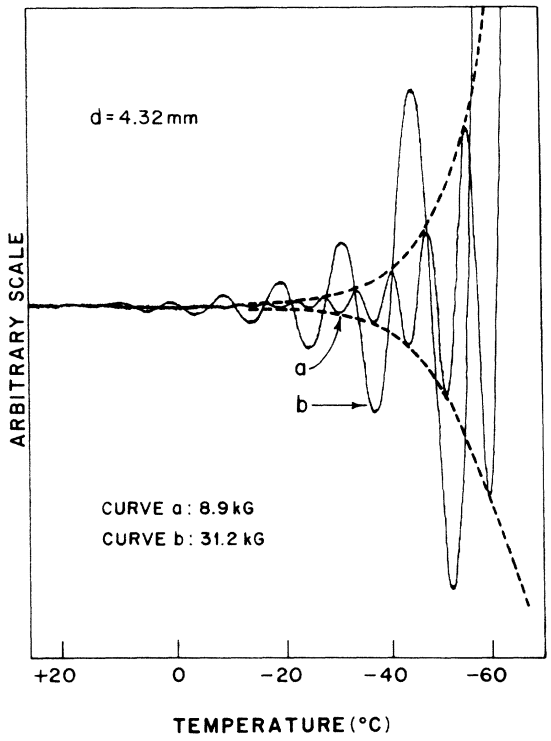

FIG. 3. Recorder traces of helicon interference in pure InSb as a function of temperature at two fixed fields. The x axis was obtained by the output of a thermocouple in contact with the specimen. The Rayleigh patterns are periodic in $n_i^{1/2}$, providing a direct, quick, and precise method of determining the temperature dependence of the carrier concentration. Note the characteristic difference in period and losses for the two cases. The envelope (indicated by dashed lines for the lower field curve) provides a simultaneous measurement of the temperature variation of helicon damping.

the variation of n_i. Interference patterns obtained as a function of temperature at fixed B are shown in Fig. 3. Such patterns, periodic in $n_i^{1/2}$, provide an automatic recording of the variation of n_i with temperature. The results obtained from these plots, as well as similar data covering the range 220 to 400°K, are in excellent agreement with the dependence $T^3 \times \exp(-0.26/kT)$. The temperature dependence of damping is also contained in the data, although, as pointed out above, a more satisfactory model is required for a detailed quantitative interpretation of the envelope.

The author wishes to thank Dr. A. J. Strauss of Lincoln Laboratory for the InSb samples, and Dr. R. W. Arndt and Dr. R. C. Milward for valuable discussions. He is greatly indebted to Mr. P. Colluccio for his highly skilled assistance in all phases of the experimental work.

*Supported by the U. S. Air Force Office of Scientific Research.

[1]For a comprehensive review of the field, see R. Bowers and M. C. Steele, Proc. IEEE 25, 1105 (1964).

[2]A. Libchaber and R. Veilex, Phys. Rev. 127, 774 (1962); Proceedings of the International Conference on the Physics of Semiconductors. Exeter, July, 1962 (The Institute of Physics and the Physical Society, London, 1962), p. 138.

[3]J. K. Furdyna, thesis, Northwestern University, 1960 (unpublished); see also J. K. Furdyna and S. Broersma, Bull. Am. Phys. Soc. 4, 410 (1959).

[4]G. A. Williams and G. E. Smith, IBM J. Res. Develop. 8, 276 (1964).

[5]C. C. Grimes and S. J. Buchsbaum, Phys. Rev. Letters 12, 357 (1964).

[6]A detailed description and analysis of the technique will be published elsewhere.

[7]J. K. Furdyna and S. Broersma, Phys. Rev. 120, 1995 (1960), Eq. (8).

[8]Similar results have very recently been obtained by R. W. Arndt of this laboratory by a modified nmr technique in the radio-frequency range (private communication).

[9]T. S. Moss, in Progress in Semiconductors, edited by A. F. Gibson (John Wiley & Sons, Inc., New York, 1960), Vol. 5, pp. 210-211.

[10]E. N. Adams and T. D. Holstein, J. Phys. Chem. Solids 10, 254 (1959).